

Nanosize-Induced Drastic Drop in Equilibrium Hydrogen Pressure for Hydride Formation and Structural Stabilization in Pd–Rh Solid-Solution Alloys

Hirokazu Kobayashi,^{*,†,‡,§} Hitoshi Morita,[‡] Miho Yamauchi,^{‡,||} Ryuichi Ikeda,^{†,‡,⊥}
Hiroshi Kitagawa,^{*,†,‡,§,⊥,⊗} Yoshiki Kubota,[#] Kenichi Kato,^{∇,◆} Masaki Takata,^{∇,◆} Shoichi Toh,^{⊥,+}
and Syo Matsumura^{⊥,⊗,+||}

[†]Division of Chemistry, Graduate School of Science, Kyoto University, Kitashirakawa-Oiwakecho, Sakyo-ku, Kyoto 606-8502, Japan

[‡]Department of Chemistry, Faculty of Science, Kyushu University, Hakozaki, Fukuoka 812-8581, Japan

[§]Institute for Integrated Cell-Material Sciences (iCeMS), Kyoto University, Yoshida, Sakyo-ku, Kyoto 606-8501, Japan

^{||}International Institute for Carbon Neutral Energy Research (I²CNER), [⊗]INAMORI Frontier Research Center, ⁺Research Laboratory of High-Voltage Electron Microscope, and [#]Department of Applied Quantum Physics and Nuclear Engineering, Kyushu University, Motoooka 744, Nishi-ku, Fukuoka 819-0395, Japan

[⊥]JST CREST, Sanbancho 5, Chiyoda-ku, Tokyo 102-0075, Japan

[#]Department of Physical Science, Graduate School of Science, Osaka Prefecture University, Sakai, Osaka 599-8531, Japan

[∇]RIKEN SPring-8 Center, 1-1-1 Kouto, Sayo-cho, Sayo-gun, Hyogo 679-5148, Japan

[◆]Japan Synchrotron Radiation Research Institute, 1-1-1 Kouto, Sayo-cho, Sayo-gun, Hyogo 679-5198, Japan

Supporting Information

ABSTRACT: We have synthesized and characterized homogeneous solid-solution alloy nanoparticles of Pd and Rh, which are immiscible with each other in the equilibrium bulk state at around room temperature. The Pd–Rh alloy nanoparticles can absorb hydrogen at ambient pressure and the hydrogen pressure of Pd–Rh alloys for hydrogen storage is dramatically decreased by more than 4 orders of magnitude from the corresponding pressure in the metastable bulk state. The solid-solution state is still maintained in the nanoparticles even after hydrogen absorption/desorption, in contrast to the metastable bulks which are separated into Pd and Rh during the process.

The hydride of palladium-based alloys has been intensively investigated in various fields of fundamental science and technology for developing hydrogen storage, purification filters, isotope separation, and electrodes for metal hydride batteries.¹ In particular, Pd–Rh has been studied as a hydrogen-storage material for many years.^{1,2} A crucial problem in the Pd–Rh system is that Pd and Rh are immiscible with each other in the thermal equilibrium over the entire composition range; rather, the alloys form a segregated domain structure at around room temperature.³ Consequently, alloys composed of Pd and Rh have been obtained only as a metastable state by quenching from extremely high temperatures above 1000 K,^{2a–c} and the obtained alloys absorb a larger amount of hydrogen than does Pd, which has a high hydrogen-storage ability.¹ However, the equilibrium hydrogen pressure for hydride formation (Pd–Rh–H) increases greatly with increasing Rh content and the pressure reaches as high as 1000 MPa by 50 atom %

replacement of Pd with Rh atoms.^{2d} Furthermore, the metastable Pd–Rh alloys are not stable and are readily separated into two phases of Pd and Rh upon hydrogen absorption/desorption.^{2a,b}

It is well-known that metal nanoparticles show different chemical and physical properties from bulk metals because of their unique properties, based on their high surface-to-volume ratio and quantum size effects.⁴ In particular, nanosized metals show characteristic phase behaviors, such as a lowering of their melting point⁵ or spontaneous alloying.⁶ Because the hydrogen-storage properties of a metal are strongly related to its electronic state, metal nanoparticles are expected to show specific hydrogen-storage properties that depend on their structure or size.⁷ Here, we report the nanosize-induced stabilization of solid-solution alloys where Pd and Rh are homogeneously mixed at the atomic level and a dramatic lowering of the equilibrium hydrogen pressure by more than 4 orders of magnitude from the corresponding pressure in the bulk state. Furthermore, the solid-solution state is maintained in the nanoparticles even after hydrogen absorption/desorption, although the bulk alloys are separated into two phases of Pd and Rh during the process.

Poly(*N*-vinyl-2-pyrrolidone) (PVP)-protected Pd–Rh nanoparticles were prepared by a polyol method. An aqueous solution of Pd(NO₃)₂ and RhCl₃ was added to an ethylene glycol solution with PVP, and the mixture was heated at 368 K for 1 h with vigorous stirring. The atomic percentage of Rh in the Pd–Rh nanoparticles was estimated to be 46% by ICP–MS. A TEM image of the obtained Pd–Rh nanoparticles is shown in Figure 1a. It was found that the synthesized

Received: May 24, 2012

Published: July 16, 2012

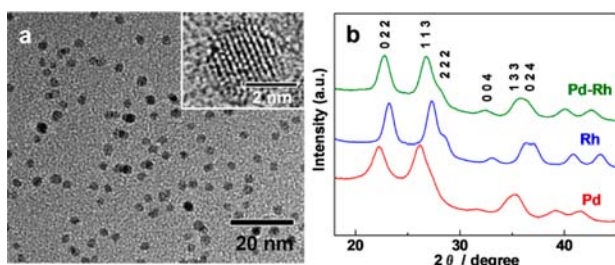


Figure 1. (a) TEM image of Pd–Rh nanoparticles. (b) XRD patterns of Pd, Pd–Rh, and Rh nanoparticles.

nanoparticles have a good crystalline structure and the mean diameter was estimated to be 2.9 ± 0.6 nm. Pd–Rh nanoparticles showed a powder X-ray diffraction (XRD) pattern originating from a single face-centered cubic (fcc) lattice (Figure 1b). The crystal size was estimated to be 2.5 nm from the Scherrer equation, which is consistent with the mean diameter from the TEM image. The diffraction peaks of Pd–Rh nanoparticles were observed between those of Pd and Rh nanoparticles, and the lattice constant of Pd–Rh nanoparticles was estimated to be 3.880 Å from the Le Bail fitting of the diffraction pattern, while those of Pd and Rh nanoparticles were 3.969 and 3.802 Å, respectively. These results strongly support the formation of an atomic-level Pd–Rh alloy over the whole inside of the particle.

We also investigated the elemental distribution of Pd and Rh in Pd–Rh nanoparticles. Figure 2a shows a high-angle annular

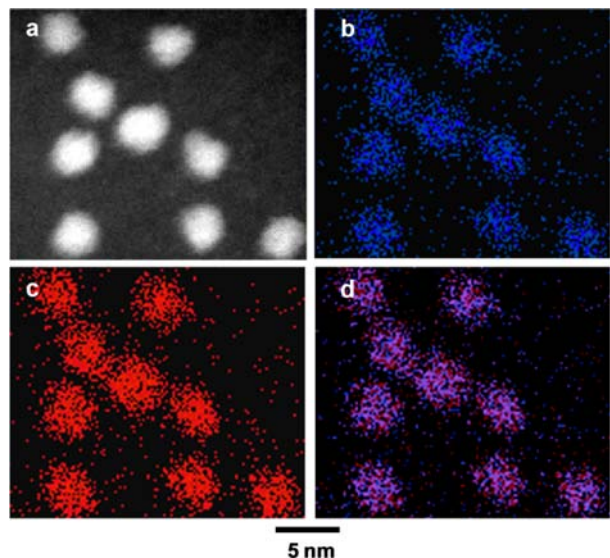


Figure 2. (a) HAADF–STEM image, (b) Pd–L STEM–EDX map, and (c) Rh–L STEM–EDX map of Pd–Rh nanoparticles. (d) The reconstructed overlay image of the maps shown in (b) and (c) (blue, Pd; red, Rh).

dark-field STEM (HAADF–STEM) image. Figures 2b and 2c show the corresponding Pd–L and Rh–L STEM–EDX maps, respectively. Figure 2d presents an overlay map of the Pd and Rh chemical distribution. These mapping data show that the obtained Pd–Rh nanoparticles form a homogeneous solid-solution alloy, where Pd and Rh are mixed at the atomic level.

It is known that hydrogen atoms permeate inside a metal or alloy lattice as individual atoms, and these interstitial hydrogen atoms produce an expansion in the metal lattice.¹ To elucidate

the lattice expansion following hydrogen absorption in Pd–Rh nanoparticles, we performed in situ XRD measurements at the BL02B2 beamline in SPring-8.⁸ As shown in Figure 3, the

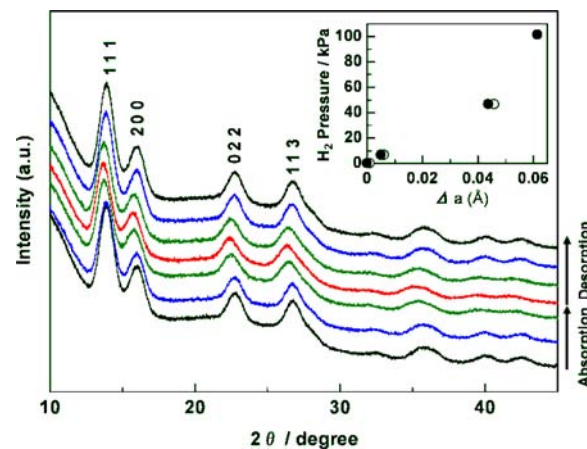


Figure 3. In situ powder XRD patterns of Pd–Rh nanoparticles upon the process of hydrogen absorption/desorption. Black, blue, green, and red lines correspond to XRD patterns measured under vacuum, 6.6, 46.6, and 101.3 kPa, respectively. Inset shows the increase in the lattice constant (Δa) estimated from the Le Bail fitting of the diffraction patterns on hydrogen absorption/desorption. Closed and open circles show the lattice constants upon the process of hydrogen absorption and desorption, respectively.

position of the diffraction peaks of the Pd–Rh nanoparticles shifted continuously to lower angles in response to increasing hydrogen pressure. The hydrogen-pressure dependence of the lattice constants was determined from the Le Bail fitting of the diffraction patterns, and the change in lattice constant (Δa) with the absorption/desorption of hydrogen is shown in Figure 3 inset. During the process of hydrogen absorption, the lattice constants increased with increasing hydrogen pressure for the Pd–Rh nanoparticles, which indicates that the Pd–Rh atoms within the lattice are forced apart. This behavior can be the consequence of hydrogen atoms penetrating the inside of the Pd–Rh lattice and expanding it. The lattice constant for a hydrogen pressure of 101.3 kPa at 303 K is increased by 0.06 Å relative to the value under vacuum. The lattice constant decreases with hydrogen desorption, and the lattice constant returns to the same value as in the pristine sample. The change in lattice constant (Δa) with the absorption/desorption of hydrogen suggests the occurrence of hydrogen-storage capability in Pd–Rh alloys at a mere 101.3 kPa induced by a nanosize effect.

We performed solid-state ^2H NMR measurements to investigate the states of ^2H in Pd–Rh solid-solution nanoparticles. The sharp lines at around 0 ppm and broad absorption line were observed for Pd–Rh nanoparticles (Figure 4a). In the spectrum for $^2\text{H}_2$ gas (Figure 4d), only a sharp line at 3 ppm was observed. By comparison of these spectra, it is reasonable to attribute the sharp components in the spectrum of the Pd–Rh particle to free deuterium gas ($^2\text{H}_2$) or deuterium atoms diffusing and/or exchanging with free deuterium on the particles' surface, and the broad component to absorbed deuterium atoms (^2H) in the particles. It is reported that the absorption lines of deuterium absorbed inside the lattices of Rh and Pd nanoparticles were observed at -108 and 36 ppm, respectively (Figure 4b,c).^{7a,b} The broad absorption line centered at ca. -30 ppm, originating from ^2H inside the Pd–

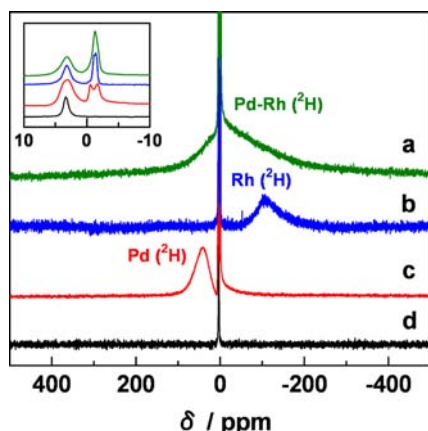


Figure 4. Solid-state ^2H NMR spectra for the samples of (a) Pd–Rh, (b) Rh, (c) Pd nanoparticles under 86.7 kPa of deuterium gas at 303 K, and (d) $^2\text{H}_2$ gas at 303 K. Inset shows expanded spectra.

Rh lattice, covers the range containing peaks for Pd and Rh nanoparticle samples (Figure 4a). These specific chemical shifts imply a difference in the electron density around the ^2H nuclei that is caused by changes in the occupancies of valence electrons as a result of hybridization of the valence bands.⁹ The specific chemical shift of Pd–Rh nanoparticles also demonstrates that atomic-level alloying occurs in the Pd–Rh system and deuterium in the nanoparticles perceives the different potentials depending on the metal species. It should be again noted that Pd–Rh nanoparticles absorb hydrogen in so low pressure as 101.3 kPa, although bulk Pd–Rh does not have hydrogen-storage capability at this pressure.

We measured hydrogen pressure–composition (PC) isotherms for the Pd–Rh solid-solution nanoparticles at 303 K. As shown in Figure 5, the total amounts of hydrogen

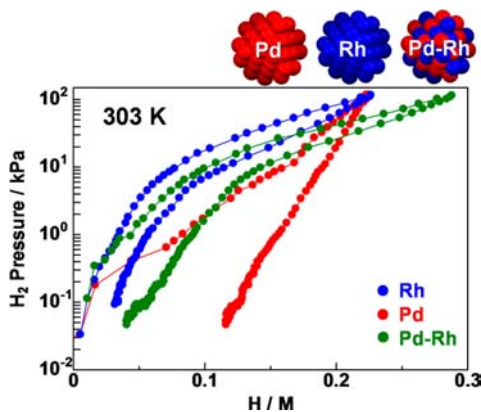


Figure 5. PC isotherms of Rh (blue), Pd (red), and Pd–Rh (green) nanoparticles. H/M means the number of hydrogen atoms divided by the total number of metal atoms.

concentration H/M at 101.3 kPa were 0.22, 0.23, 0.29 H/M for Pd, Rh, Pd–Rh nanoparticles, respectively, which demonstrates that the atomic-level Pd–Rh alloying results in a larger amount of hydrogen storage in Pd–Rh nanoparticles. It is well-known that the hydrogen concentration increases with the number of 4d-band holes.¹ A relationship between band filling and hydrogen concentrations has been reported in the case of Pd–Rh bulk alloys.^{1,2c} The amount of 4d-band holes of Pd–Rh bulk alloys at the Fermi level increases by mixing a Rh

atom, which has one less electron than the Pd atom; thereby, the hydrogen concentration of Pd–Rh bulk alloys increases with increasing Rh content. In our experimental results, the increase in the hydrogen concentrations originates from the band-filling control.

Bulk Pd–Rh alloy existing as a metastable state is known to absorb hydrogen at the extremely high pressure of 1000 MPa.^{2d} Interestingly, the Pd–Rh alloy nanoparticles in this report can absorb hydrogen even at 101.3 kPa, that is, the H_2 pressure for hydride formation in the present Pd–Rh nanoparticles is decreased by more than 4 orders of magnitude from the corresponding pressure in the bulk state. To investigate the origin of specific hydrogen storage induced by a nanosize effect for the Pd–Rh system, the temperature dependence of the plateau pressure of the absorption isotherms was examined at a hydrogen concentration of $H/M = 0.25$.¹⁰ From the van't Hoff plots of H_2 , the enthalpy $-\Delta H_{\alpha\rightarrow\beta}$ and entropy $\Delta S_{\alpha\rightarrow\beta}$ changes were estimated to be $-22.6 \text{ kJ (H}_2 \text{ mol)}^{-1}$ and $-71.1 \text{ J (H}_2 \text{ mol)}^{-1} \text{ K}^{-1}$, respectively. In bulk Pd–Rh, the enthalpy $-\Delta H_{\alpha\rightarrow\beta}$ change tends to decrease with increasing Rh contents and the change is reported to be $-19.4 \text{ kJ (H}_2 \text{ mol)}^{-1}$ for the bulk with Rh-25 atom %.^{2e} The relatively large enthalpy $-\Delta H_{\alpha\rightarrow\beta}$ change of the nanoparticles implies that the nanosize provides favorable environment to form stable hydrides. The entropy $\Delta S_{\alpha\rightarrow\beta}$ change during the hydride formation comes mainly from the entropy loss of hydrogen gas,¹¹ and the value of the entropy change is known to be basically constant for bulk hydrogen storage alloys.¹ In fact, the entropy $\Delta S_{\alpha\rightarrow\beta}$ change of Pd–Rh bulks with Rh-5–25 atom % is reported to be -93 to $-95 \text{ J (H}_2 \text{ mol)}^{-1} \text{ K}^{-1}$.^{2e} The smaller $-\Delta S_{\alpha\rightarrow\beta}$ value in the nanoparticles indicates that hydrogen atoms possess a relatively larger entropy in nanoparticles than in bulk Pd–Rh. In other words, hydrogen atoms in the nanoparticles retain a part of the freedom in the gaseous state, implying that atomic arrangements in nanoparticles are statically or dynamically disordered. A more important consideration is that a small loss of entropy causes hydride formation under a low hydrogen pressure.

It has been reported that the metastable bulk Pd–Rh solid solutions easily separates into two phases of Pd and Rh upon applying hydrogen treatment.^{2a,b,10} In contrast, the solid-solution state is still maintained in the nanoparticles before/after the measurements of PC isotherms or the H_2 treatment.¹⁰ The stable Pd–Rh mixture in the nanoparticles may allow not only for a facile and efficient hydrogen absorption/desorption performance, but also for effective catalysts in various reactions related to hydrogen.

In summary, we have synthesized and characterized size-controlled alloy nanoparticles where Pd and Rh are homogeneously mixed at the atomic level by a polyol method. The Pd–Rh alloy nanoparticles can absorb hydrogen at ambient pressure without separation into two phases of Pd and Rh and the nanosize contributed to the drastic drop in the equilibrium hydrogen pressure for hydride formation by more than 4 orders of magnitude from the corresponding pressure in the bulk state. The new findings in this report provide valuable insight for further developments of hydrogen-storage materials. In addition, these successfully obtained alloys are expected to show high activity or high durability as a catalyst for organic synthesis or in various applications, as a result of the mixing of Pd and Rh at the atomic level.

■ ASSOCIATED CONTENT

■ Supporting Information

Experimental details, PC isotherms, TEM images, XRD patterns and HAADF-STEM images. This material is available free of charge via the Internet at <http://pubs.acs.org>.

■ AUTHOR INFORMATION

Corresponding Author

hkobayashi@kuchem.kyoto-u.ac.jp; kitagawa@kuchem.kyoto-u.ac.jp

Notes

The authors declare no competing financial interest.

■ ACKNOWLEDGMENTS

This work was partly supported by the Grants-in-Aid for the Global COE Program, "Science for Future Molecular Systems" and Elements Science and Technology Project from the MEXT, Japan and by the Asahi Glass Foundation.

■ REFERENCES

- (1) Alefeld, G.; Völkl, J., Eds.; *Hydrogen in Metals II*; Springer: Berlin, Heidelberg, 1978.
- (2) (a) Noh, H.; Flanagan, T. B.; Cerundolo, B.; Craft, A. *Scr. Metall. Mater.* **1991**, *25*, 225. (b) Noh, H.; Clewley, J. D.; Flanagan, T. B.; Craft, A. P. *J. Alloys Compd.* **1996**, *240*, 235. (c) Noh, H.; Clewley, J. D.; Flanagan, T. B.; Craft, A. P. *Int. J. Hydrogen Energy* **2000**, *25*, 853. (d) Baranowski, B.; Majchrzak, S.; Flanagan, T. B. *J. Phys. Chem.* **1973**, *77*, 35. (e) Noh, H.; Luo, W.; Flanagan, T. B. *J. Alloys Compd.* **1993**, *196*, 7.
- (3) Tripathi, S. N.; Bharadwaj, S. R. *J. Phase Equilib.* **1994**, *15*, 208.
- (4) (a) Roduner, E. *Chem. Soc. Rev.* **2006**, *35*, 583. (b) Kubo, R. *J. Phys. Soc. Jpn.* **1962**, *17*, 975. (c) Marzke, R. F. *Catal. Rev.—Sci. Eng.* **1979**, *19*, 43. (d) Schmid, G. *Cluster & Colloids: From Theory to Application*; VCH: Weinheim, 1994. (e) Henglein, A. *Chem. Rev.* **1989**, *89*, 1861. (f) Bawendi, M. G.; Steigerwald, M. L.; Brus, L. E. *Annu. Rev. Phys. Chem.* **1990**, *41*, 477.
- (5) (a) Koga, K.; Ikeshoji, T.; Sugawara, K. *Phys. Rev. Lett.* **2004**, *92*, 115507–1–4. (b) Zhang, M.; Efremov, M. Y.; Schiettekatte, F.; Olson, E. A.; Kwan, A. T.; Lai, S. L.; Wisleder, T.; Greene, J. E.; Allen, H. *Phys. Rev. B* **2000**, *62*, 10548. (c) Blackman, M.; Sambles, J. R. *Nature* **1970**, *226*, 938.
- (6) (a) Shibata, T.; Bunker, B. A.; Zhang, Z.; Meisel, D.; Vardeman, C. F.; Gezelter, J. D. *J. Am. Chem. Soc.* **2002**, *124*, 11989. (b) Ouyang, G.; Tan, X.; Wang, C. X.; Yang, G. W. *Chem. Phys. Lett.* **2006**, *420*, 65. (c) Yasuda, H.; Mori, H.; Komatsu, M.; Takeda, K. *J. Appl. Phys.* **1993**, *73*, 1100. (d) Yasuda, H.; Mori, H. *Phys. Rev. Lett.* **1992**, *69*, 3747. Heidelberg, 1978
- (7) (a) Kobayashi, H.; Yamauchi, M.; Kitagawa, H.; Kubota, Y.; Kato, K.; Takata, M. *J. Am. Chem. Soc.* **2008**, *130*, 1818. (b) Kobayashi, H.; Yamauchi, M.; Kitagawa, H.; Kubota, Y.; Kato, K.; Takata, M. *J. Am. Chem. Soc.* **2011**, *133*, 11034. (c) Kobayashi, H.; Yamauchi, M.; Kitagawa, H. *J. Am. Chem. Soc.* **2012**, *134*, 6893. (d) Kobayashi, H.; Yamauchi, M.; Kitagawa, H.; Kubota, Y.; Kato, K.; Takata, M. *J. Am. Chem. Soc.* **2008**, *130*, 1828. (e) Kobayashi, H.; Yamauchi, M.; Kitagawa, H.; Kubota, Y.; Kato, K.; Takata, M. *J. Am. Chem. Soc.* **2010**, *132*, 5576. (f) Kobayashi, H.; Yamauchi, M.; Ikeda, R.; Kitagawa, H. *Chem. Commun.* **2009**, 4806. (g) Yamauchi, M.; Kobayashi, H.; Kitagawa, H. *ChemPhysChem* **2009**, *10*, 2566. (h) Sun, Y.; Tao, Z.; Chen, J.; Herricks, T.; Xia, Y. *J. Am. Chem. Soc.* **2004**, *126*, 5940. (i) Shao, H.; Xu, H.; Wang, Y.; Li, X. *J. Solid State Chem.* **2004**, *177*, 3626. (j) Suleiman, M.; Jisrawi, N. M.; Dankert, O.; Reetz, M. T.; Bahtz, C.; Kirchheim, R.; Pundt, A. *J. Alloys Compd.* **2003**, *356–357*, 644. (k) Bogdanov, B.; Felderhoff, M.; Kaskel, S.; Pommerin, A.; Schlichte, K.; Schüth, F. *Adv. Mater.* **2003**, *15*, 1012. (l) Hanneken, J. W.; Baker, D. B.; Conradi, M. S.; Eastman, J. A. *J. Alloys Compd.* **2002**, *330–332*, 714.

(8) (a) Nishibori, E.; Takata, M.; Kato, K.; Sakata, M.; Kubota, Y.; Aoyagi, S.; Kuroiwa, Y.; Yamakata, M.; Ikeda, N. *Nucl. Instrum. Methods Phys. Res., Sect. A* **2001**, *467–468*, 1045.

(9) Nascente, P. A. P.; de Castro, S. G. C.; Landers, R.; Kleiman, G. *Phys. Rev. B* **1991**, *43*, 4659.

(10) See Supporting Information.

(11) Fukai, Y. *The Metal-Hydrogen System: Basic Bulk Properties*, 2nd ed.; Springer-Verlag: Berlin, 2005; p 9.